

PAPER • OPEN ACCESS

Bending capacity of multi-layered FRP pipelines during offshore installation

To cite this article: Dimitrios Pavlou 2021 *IOP Conf. Ser.: Mater. Sci. Eng.* **1201** 012039

View the [article online](#) for updates and enhancements.

You may also like

- [Influence of anchorage systems on externally-bonded CFRP sheets used for flexural strengthening](#)
B Al-Atta, R Kalfat, R Al-Mahaidi et al.
- [Study on the quality of FRP fishing vessel based on improved Fishbone Chart](#)
J H Sui, Y F Yu, Q F Du et al.
- [State-of-the-Art on Fire Resistance Aspects of FRP Reinforcing Bars](#)
Kostiantyn Protchenko, Elzbieta Szmigiera, Marek Urbanski et al.



The Electrochemical Society
Advancing solid state & electrochemical science & technology

241st ECS Meeting

May 29 – June 2, 2022 Vancouver • BC • Canada

Abstract submission deadline: Dec 3, 2021

Connect. Engage. Champion. Empower. Accelerate.
We move science forward



Submit your abstract



Bending capacity of multi-layered FRP pipelines during offshore installation

Dimitrios Pavlou

Department of Mechanical and Structural Engineering and Material Science, Faculty of Science and Technology, University of Stavanger, Stavanger, Norway

* Contact E-mail: dimitrios.g.pavlou@uis.no

Abstract. The Fiber Reinforced Polymeric (FRP) pipelines have higher strength than steel, and excellent fatigue behavior and corrosion resistance. Because of their superior performance in mechanical loads and corrosive environment, they are a good choice for offshore applications. Since FRP materials are anisotropic and the pipelines are multilayered, the calculation of stresses is difficult. Stress analysis can be performed numerically with the aid of commercial software packages. However, the numerical solutions are approximate and the parametric study is problematic. In the present work, an analytical solution for bending stress calculation of multilayered FRP pipelines during offshore installation is presented. Typical examples are solved and bending capacity of multilayered FRP pipelines versus the fiber orientation angle and number of layers is provided and discussed.

Keywords: FRP materials, flexible pipelines, anisotropic materials, offshore structures

1. Introduction

The loading conditions of a composite pipeline have fundamental importance for its dimensioning. Underestimation of the fundamental sizing of a pipeline can cause failure with catastrophic environmental, economic and geopolitical consequences. On the other hand, as the length of a pipeline (especially for oil and gas transmission) is extremely large (because it passes very often through countries and oceans) small inadequate overestimation in sizing (eg. in the wall thickness) can result to critical consequences in the competition of the project. Therefore, the type of loads to be considered is a key factor for a successful design. The loads affecting the dimensions of a composite pipeline are classified in the following two main categories: a) Installation loads, and b) Operation loads.

1.1. Installation loads

Depending on the selected installation method, the installation loads are very often more critical for the pipeline dimensioning than the operation loads [1, 2]. For the case of offshore pipelines, the installation methods can be (a) S-Lay (Figure 1), (b) J-Lay (Figure 2), (c) Towing (Figures 3 (a)-(c)). In the case of the continental pipelines, the pipes are mostly embedded in the soil (Figure 4), because of their sensitivity in ultraviolet radiation. The installation of on-shore pipelines is taking place by using movable cranes and compaction machines.



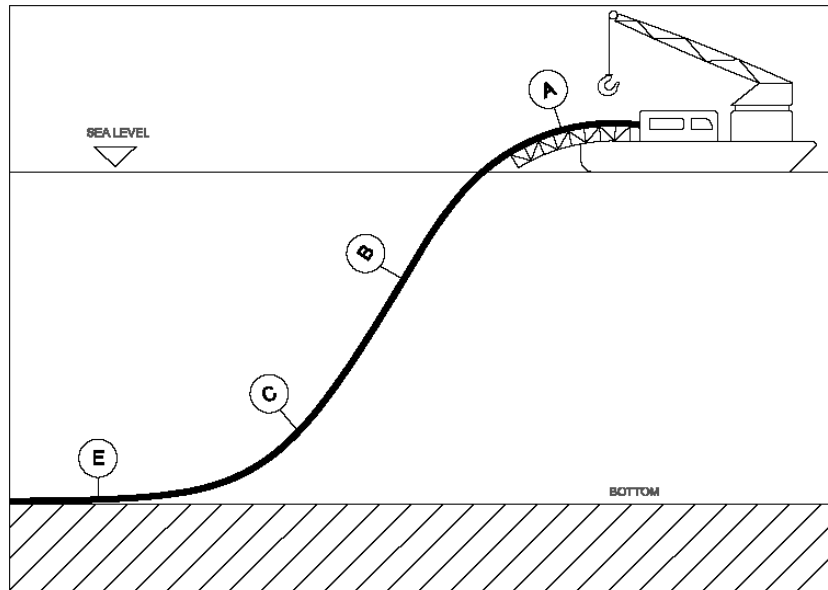
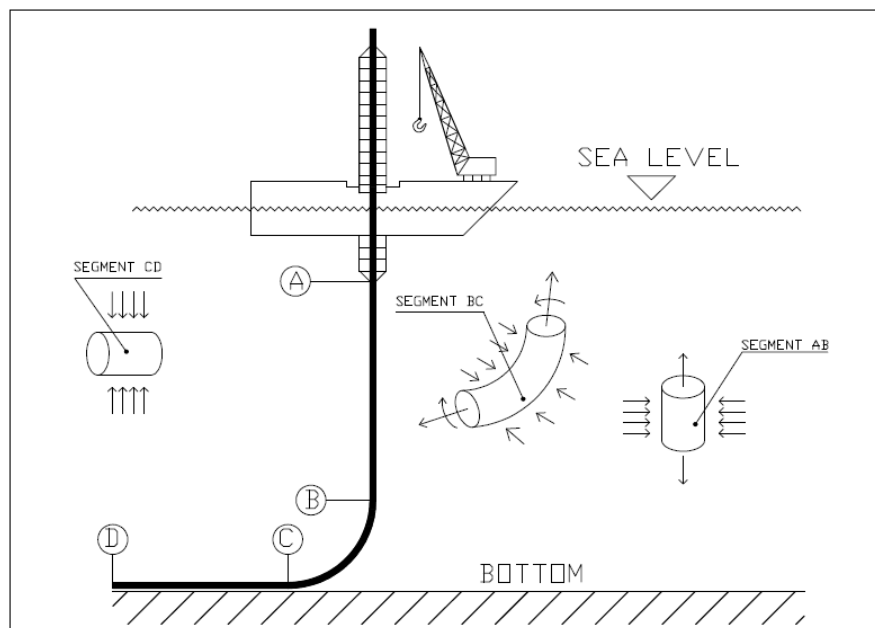
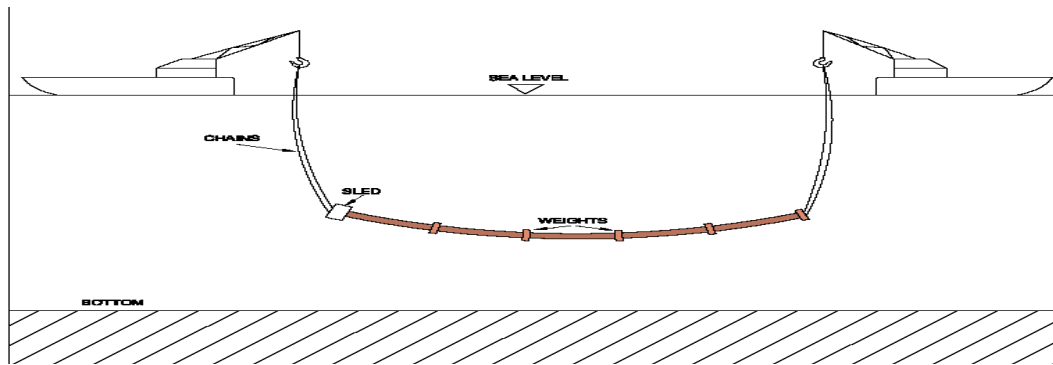


Figure 1. S-Lay installation process

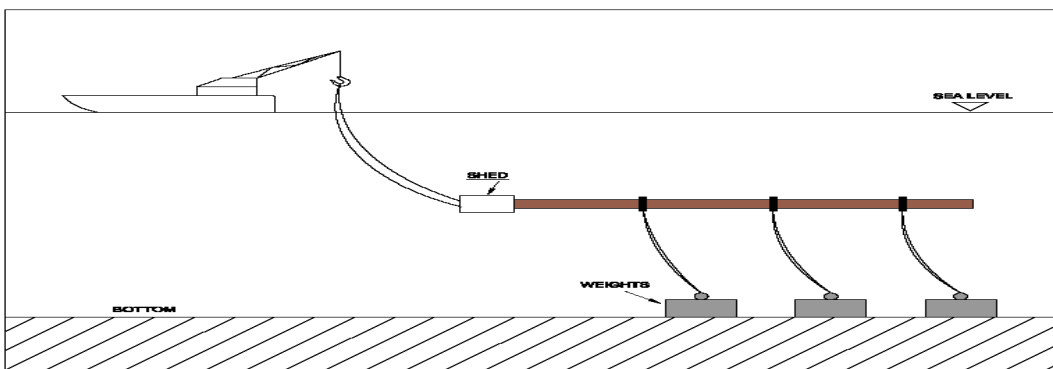


(b)

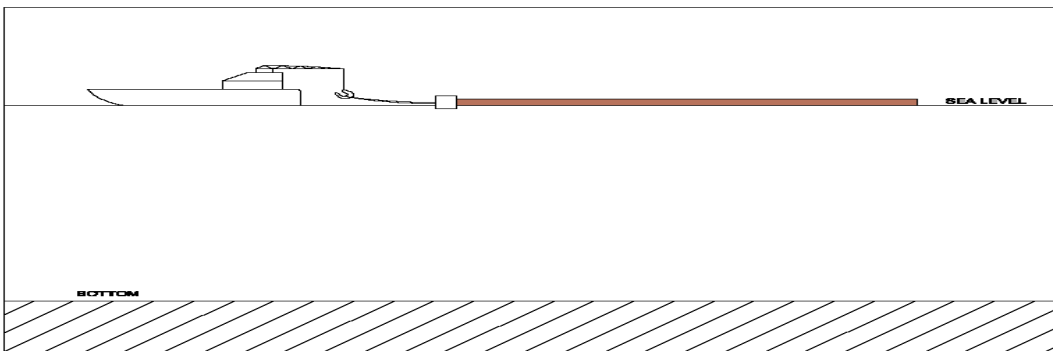
Figure 2. J-lay installation process



(a)



(b)



(c)

Figure 3. (a) Mid depth tow, (b) Off-bottom tow, (c) Surface tow

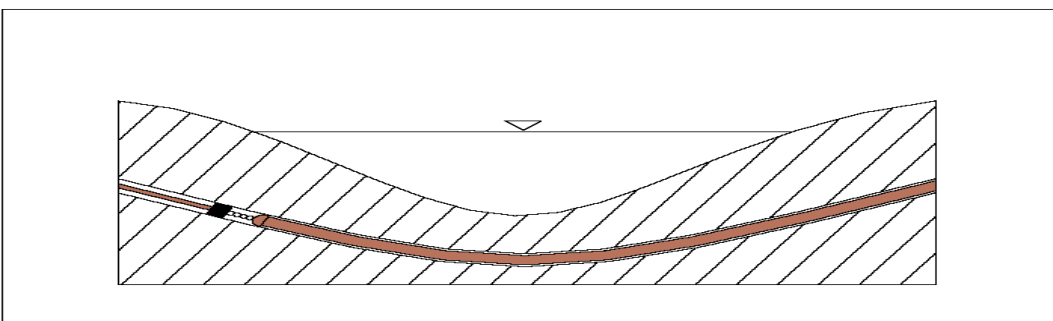


Figure 4. Installation of a pipeline within soil

During above (offshore and on shore) installation procedures the pipeline is subjected to pseudo-static loads of the following loading cases: i) Bending, ii) Axial Tension, iii) External pressure, iv) Combination of bending and axial-tension, v) Combination of external pressure and axial-tension, vi) Combination of bending, external pressure and axial tension, vii) Torsion (e.g. during the turn on the sea of the installation ship), viii) Combination of Torsion, Bending, Axial Tension and External Pressure. Above loading cases are causing plane stress conditions in composite pipes wall. Therefore, the stress state for every lamina has to be analyzed by a failure criterion. Moreover, the external pressure, bending, torsion and their combinations can cause local buckling into the wall of the composite pipe. The above-described loading cases are summarized in Table 1.

1.2. Operation loads

During service, composite pipelines can be subjected to static, pseudo-static, or dynamic loading conditions at ordinary or elevated temperatures. During static conditions the loads are keeping continuously constant values, while during pseudo-static situations their changes are taking place very slowly, assuming every time static conditions. During static or pseudo-static loading cases, the stresses can be produced due to e.g.: a) internal pressure, b) deformation of the pipe due to its self-weight and supporting method, c) thermal stresses due to temperature gradients, d) creep effects due to uniform (or variable) elevated temperatures, e) moisture stain effects and f) soil-pipe interactions for underground pipes. The dynamic loads can be a) vibrations because of e.g., hydrodynamic forces due to internal axial flow or external cross flow (fluid-pipe interactions), b) impact due to e.g., fluid hammer or c) local impact due to foreign object. During variable loading conditions the material mechanisms yielding failure are different than those taking place during static or pseudo-static loads. Therefore, the failure criteria developed for static loads are inadequate for designing purposes. In this case the designer has to use fatigue damage accumulation rules in order to ensure the sustainability of the pipeline for the specified life.

Table 1. Classification of loads acting on composite pipelines

| | Loading types | Checks | | | |
|--------------------|---|-------------------|----------|---------|-------|
| | | Failure criterion | Buckling | Fatigue | Creep |
| Installation loads | Bending | + | + | | |
| | Axial Tension | + | | | |
| | External Pressure | + | + | | |
| | Combination of bending and axial Tension | + | + | | |
| | Combination of external pressure and axial tension | + | + | | |
| | Combination of bending, external pressure and axial tension | + | + | | |
| | Torsion | + | + | | |
| | Combination of torsion, bending axial tension and external pressure | + | + | | |
| Operation loads | Constant internal fluid pressure | + | | | + |
| | Fluctuation internal fluid pressure | + | | + | |
| | Hydrodynamic forces due to internal axial flow | + | | + | |
| | Hydrodynamic forces due to external cross flow | + | | + | |

| | | | |
|--|---|---|---|
| Impact pressure due to fluid hammer | + | | |
| Thermal stresses due to temperature gradients | + | + | + |
| Uniform elevated temperature effects | | | + |
| Moisture strain effects | + | | |
| External pressure due to pipe-soil interaction (forces due to soil weight and road or rail crossings of underground pipelines) | + | + | |
| Bending due to differential settlement of soil (of underground pipelines) | + | + | |
| Local impact by foreign objects | + | | |

Moreover, for long time loading histories, especially at elevated temperatures, the designer has to take into account the deformation or possible rupture due to creep. Today, damage mechanics provides valuable theoretical tools [e.g. 3-5] for an effective design preventing fatigue or/and creep damage. Table 1 summarizes the main composite pipeline operation loads as well as the required checks for sustainable design.

The most severe loads take place during S-lay or J-lay installation. The predominant stresses during installation are the bending stresses. In the present work the Lekhnitskii formalism is used and the equilibrium equations and the compatibility and boundary conditions in the layer interfaces are used for the derivation of the analytical model. Then, the Tsai-Wu failure criterion is used for calculating the bending capacity of offshore pipelines.

2. Formulation of the problem

2.1. Failure analysis

Bending is the most common loading case of installation of a composite pipeline. During the procedure of e.g. S-Lay or J-Lay installation the pipeline has to be curved causing significant normal stresses in each lamina. Moreover, during the operation, possible free-spans on the sea floor of an offshore pipeline or possible soil settlement of an underground one can also cause bending. In most of the bending cases the determination of the allowable bending moment or the minimum radius of curvature of the deformed pipeline is usually the main target of bending analysis. Since the plastic deformation of composite materials is almost absent in their stress-strain behavior (compared to steel), the stress and deflection analysis of composite pipelines will be based only on elasticity equations.

The available data of the designer in order to perform stress and failure analysis of a pipeline under bending are:

- (1) The engineering properties of the used material in the principal coordinate system, i.e.:
 - a. The modulus of elasticity E_1, E_2
 - b. The Poisson's ratio ν_{12}
 - c. The shear modulus G_{12}
 - d. The longitudinal tensile strength σ_1^T
 - e. The longitudinal compressive strength σ_1^C
 - f. The transverse tensile strength σ_2^T
 - g. The transverse compressive strength σ_2^C
 - h. The in-plane shear strength τ_{12}^F

- (2) The fiber orientation θ of each layer and the corresponding stacking sequence of the
- (3) The thickness h of each layer
- (4) The internal diameter D of the pipe.

After the selection of the material, the data $l(a)-(h)$ can easily be found by existing data bases (e.g. Table 2) containing material properties. The input data (2)-(4) are design parameters to be chosen by the designer taking into account e.g., manufacturing cost parameters, the fluid supply/demand scenario, the tolerance of the pipeline for the rest loading cases, etc.

Table 2. Material properties of widely used composites [6]

| | E- Glass/Epoxy | S- Glass/Epoxy | AS/3501 Carbon/Epoxy | T300/5208 Carbon/Epoxy |
|---------------------|-------------------|-------------------|-------------------------|---------------------------|
| E_1 (GPa) | 39 | 43 | 138 | 181 |
| E_2 (GPa) | 8.6 | 8.9 | 8.96 | 10.3 |
| ν_{12} | 0.28 | 0.27 | 0.30 | 0.28 |
| G_{12} (GPa) | 3.8 | 4.5 | 7.10 | 7.17 |
| σ_1^T (MPa) | 1080 | 1280 | 1447 | 1500 |
| σ_1^C (MPa) | 620 | 690 | 1447 | 1500 |
| σ_2^T (MPa) | 39 | 49 | 51.7 | 40 |
| σ_2^C (MPa) | 128 | 158 | 206 | 246 |
| τ_{12}^F (MPa) | 89 | 69 | 93 | 68 |

3. Mathematical model

To derive a model for dimensioning of a multi-layered filament wound pipe under bending, the Lekhnitskii formalism for stress and displacements of a single-layered pipe is going to be initially used.

3.1 Single-layered pipe

According to [7], the stress distribution on a single-layered pipe is given by the following equations.

$$\sigma_r = \left[C_1 r^{n-1} - C_2 r^{-n-1} + \frac{C_3}{r} + Agr \right] \sin \varphi \quad (1)$$

$$\sigma_\varphi = \left[C_1 (n+1) r^{n-1} + C_2 (n-1) r^{-n-1} + \frac{C_3}{r} + 3Agr \right] \sin \varphi \quad (2)$$

$$\sigma_z = Ar \sin \theta - \frac{1}{S_{33}} (S_{13} \sigma_r + S_{23} \sigma_\varphi) \quad (3)$$

or

$$\sigma_z = \frac{1}{S_{33}} \left[-(S_{13} + S_{23} + nS_{23}) r^{n-1} C_1 + (S_{13} + S_{23} - nS_{23}) r^{-n-1} C_2 - (S_{13} + S_{23}) r^{-1} C_3 + (S_{33} - S_{13}g - 3S_{23}g) rA \right] \sin \varphi \quad (4)$$

$$\tau_{r\varphi} = -[r^{n-1}C_1 - r^{-n-1}C_2 + r^{-1}C_3 + grA] \cos \varphi \quad (5)$$

where [8]:

$$[S_{ij}] = [Q_{ij}]^{-1} [\alpha_{ij}] [P_{ij}] \quad (6)$$

$$[Q_{ij}] = \begin{bmatrix} 1 & 0 & 0 & 0 & 0 & 0 \\ 0 & \cos^2 \theta & \sin^2 \theta & 0 & \cos \theta \sin \theta & 0 \\ 0 & \sin^2 \theta & \cos^2 \theta & 0 & \cos \theta \sin \theta & 0 \\ 0 & 0 & 0 & \cos \theta & 0 & -\sin \theta \\ 0 & 2 \cos \theta \sin \theta & -2 \cos \theta \sin \theta & 0 & \cos^2 \theta - \sin^2 \theta & 0 \\ 0 & 0 & 0 & \sin \theta & 0 & \cos \theta \end{bmatrix} \quad (7)$$

$$[P_{ij}] = \begin{bmatrix} 1 & 0 & 0 & 0 & 0 & 0 \\ 0 & \cos^2 \vartheta & \sin^2 \vartheta & 0 & -2 \cos \vartheta \sin \vartheta & 0 \\ 0 & \sin^2 \vartheta & \cos^2 \vartheta & 0 & 2 \cos \vartheta \sin \vartheta & 0 \\ 0 & 0 & 0 & \cos \vartheta & 0 & -\sin \vartheta \\ 0 & \cos \vartheta \sin \vartheta & -\cos \vartheta \sin \vartheta & 0 & \cos^2 \vartheta - \sin^2 \vartheta & 0 \\ 0 & 0 & 0 & \sin \vartheta & 0 & \cos \vartheta \end{bmatrix} \quad (8)$$

$$[a_{ij}] = \begin{bmatrix} \frac{1}{E_2} & -\frac{\nu_{32}}{E_2} & -\frac{\nu_{21}}{E_1} & 0 & 0 & 0 \\ -\frac{\nu_{32}}{E_2} & \frac{1}{E_2} & -\frac{\nu_{21}}{E_1} & 0 & 0 & 0 \\ -\frac{\nu_{21}}{E_1} & -\frac{\nu_{21}}{E_1} & \frac{1}{E_1} & 0 & 0 & 0 \\ 0 & 0 & 0 & \frac{2(1-\nu_{32})}{E_2} & 0 & 0 \\ 0 & 0 & 0 & 0 & \frac{1}{G_{12}} & 0 \\ 0 & 0 & 0 & 0 & 0 & \frac{1}{G_{12}} \end{bmatrix} \quad (9)$$

$$g = \frac{S_{23} - S_{13}}{\beta_{11} + 2\beta_{12} + \beta_{66} - 3\beta_{22}} \quad (10)$$

$$n = \sqrt{1 + \frac{\beta_{11} + 2\beta_{12} + \beta_{66}}{\beta_{22}}} \quad (11)$$

$$\beta_{ij} = S_{ij} - \frac{S_{i3}S_{j3}}{S_{33}} \quad (12)$$

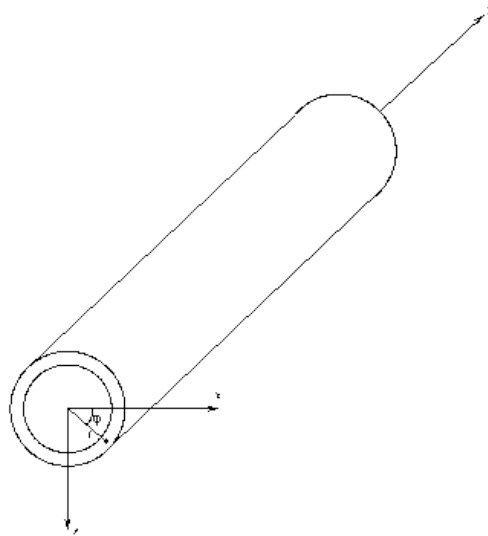


Figure 5. Geometry of a single-layered pipe

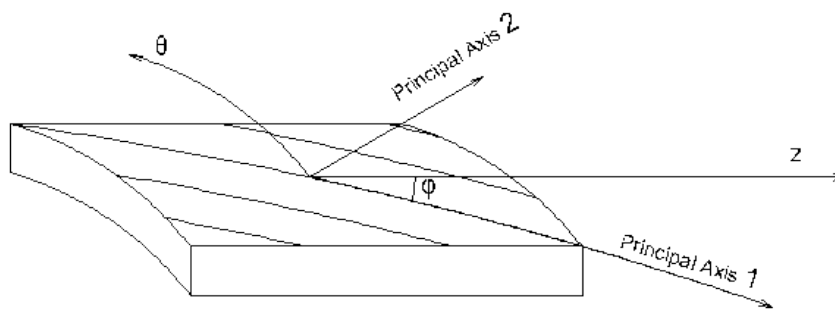


Figure 6. Coordinate systems for directions of stresses acting on a lamina

According to [e.g. 9], the strains and stresses in directions z, φ, r (Figures 5 and 6) are correlated with the following relationships:

$$\varepsilon_z = \bar{S}_{11} \sigma_z + \bar{S}_{12} \sigma_\varphi + \bar{S}_{13} \sigma_r \quad (13)$$

$$\varepsilon_\varphi = \bar{S}_{21} \sigma_z + \bar{S}_{22} \sigma_\varphi + \bar{S}_{23} \sigma_r \quad (14)$$

$$\varepsilon_r = \bar{S}_{31} \sigma_z + \bar{S}_{32} \sigma_\varphi + \bar{S}_{33} \sigma_r \quad (15)$$

$$\gamma_{r\varphi} = \frac{1}{2} \bar{S}_{44} \tau_{r\varphi} \quad (16)$$

where \bar{S}_{ij} are given in Appendix I of the Chapter 1 [9].

Taking into account the Eqs. (1)-(4), the above equations yield:

$$\begin{aligned} \varepsilon_z = \bar{S}_{11} \left\{ \frac{1}{S_{33}} \left[-(S_{13} + S_{23} + nS_{23})r^{n-1}C_1 + (S_{13} + S_{23} - nS_{23})r^{-n-1}C_2 - \right. \right. \\ \left. \left. (S_{13} + S_{23})r^{-1}C_3 + (S_{33} - S_{13}g - 3S_{23}g)rA \right] \sin \varphi \right\} + \\ \bar{S}_{12} \left\{ \left[(n+1)r^{n-1}C_1 + (n-1)r^{-n-1}C_2 + r^{-1}C_3 + 3grA \right] \sin \varphi \right\} + \\ \bar{S}_{13} \left\{ \left[r^{n-1}C_1 - r^{-n-1}C_2 + r^{-1}C_3 + grA \right] \sin \varphi \right\} \end{aligned} \quad (17)$$

or

$$\begin{aligned} \varepsilon_z = \sin \varphi \left\{ \bar{S}_{11} \frac{1}{S_{33}} \left[-(S_{13} + S_{23} + nS_{23})r^{n-1}C_1 + (S_{13} + S_{23} - nS_{23})r^{-n-1}C_2 - \right. \right. \\ \left. \left. (S_{13} + S_{23})r^{-1}C_3 + (S_{33} - S_{13}g - 3S_{23}g)rA \right] + \right. \\ \bar{S}_{12} \left[(n+1)r^{n-1}C_1 + (n-1)r^{-n-1}C_2 + r^{-1}C_3 + 3grA \right] + \\ \left. \bar{S}_{13} \left[r^{n-1}C_1 - r^{-n-1}C_2 + r^{-1}C_3 + grA \right] \right\} \end{aligned} \quad (18)$$

$$\begin{aligned} \varepsilon_\varphi = \sin \varphi \left\{ \bar{S}_{21} \frac{1}{S_{33}} \left[-(S_{13} + S_{23} + nS_{23})r^{n-1}C_1 + (S_{13} + S_{23} - nS_{23})r^{-n-1}C_2 - \right. \right. \\ \left. \left. (S_{13} + S_{23})r^{-1}C_3 + (S_{33} - S_{13}g - 3S_{23}g)rA \right] + \right. \\ \bar{S}_{22} \left[(n+1)r^{n-1}C_1 + (n-1)r^{-n-1}C_2 + r^{-1}C_3 + 3grA \right] + \\ \left. \bar{S}_{13} \left[r^{n-1}C_1 - r^{-n-1}C_2 + r^{-1}C_3 + grA \right] \right\} \end{aligned} \quad (19)$$

$$\begin{aligned} \varepsilon_r = \sin \varphi \left\{ \bar{S}_{31} \frac{1}{S_{33}} \left[-(S_{13} + S_{23} + nS_{23})r^{n-1}C_1 + (S_{13} + S_{23} - nS_{23})r^{-n-1}C_2 - \right. \right. \\ \left. \left. (S_{13} + S_{23})r^{-1}C_3 + (S_{33} - S_{13}g - 3S_{23}g)rA \right] + \right. \\ \bar{S}_{32} \left[(n+1)r^{n-1}C_1 + (n-1)r^{-n-1}C_2 + r^{-1}C_3 + 3grA \right] + \\ \left. \bar{S}_{33} \left[r^{n-1}C_1 - r^{-n-1}C_2 + r^{-1}C_3 + grA \right] \right\} \end{aligned} \quad (20)$$

$$\gamma_{r\varphi} = -\frac{1}{2} \bar{S}_{44} \cos \varphi \left[r^{n-1}C_1 - r^{-n-1}C_2 + r^{-1}C_3 + grA \right] \quad (21)$$

The above strains $\varepsilon_r, \varepsilon_\varphi, \varepsilon_z, \gamma_{r\varphi}$ can be correlated with the displacements u_r and u_φ by the following relationships [e.g. 11-13]:

$$\varepsilon_r = \frac{\partial u_r}{\partial r} \quad (22)$$

$$\varepsilon_\varphi = \frac{u_r}{r} + \frac{1}{r} \frac{\partial u_\varphi}{\partial \varphi} \quad (23)$$

$$\varepsilon_z = \frac{\partial u_z}{\partial z} \quad (24)$$

$$\gamma_{r\varphi} = \frac{1}{r} \frac{\partial u_r}{\partial \varphi} + \frac{\partial u_\varphi}{\partial r} - \frac{u_\varphi}{r} \quad (25)$$

Substitution

of eq. (20) with eq. (22) yields:

$$u_r = \int \varepsilon_r dr + F(\varphi) \quad (26)$$

or

$$\begin{aligned} u_r = & \frac{1}{2nS_{33}} r^{-n} \left[2C_2 \left(-S_{13} \bar{S}_{31} + (-1+n) S_{23} \bar{S}_{31} + S_{33} \left(\bar{S}_{32} - n \bar{S}_{32} + \bar{S}_{33} \right) \right) - \right. \\ & 2C_1 r^{2n} \left(S_{13} \bar{S}_{31} + (1+n) S_{23} \bar{S}_{31} - S_{33} \left(\bar{S}_{32} + n \bar{S}_{32} + \bar{S}_{33} \right) \right) + \\ & nr^n \left(Ar^2 \left(S_{33} \bar{S}_{31} + g \left(-\bar{S}_{31} (S_{13} + 3S_{23}) + S_{33} \left(3\bar{S}_{32} + \bar{S}_{33} \right) \right) \right) \right) + \\ & \left. + 2C_3 \left(-\bar{S}_{31} (S_{13} + S_{23}) + S_{33} \left(\bar{S}_{32} + \bar{S}_{33} \right) \right) \ln(r) \right] \sin \varphi + \\ & + F(\varphi) \end{aligned} \quad (27)$$

According to [7] the displacements should be single-valued functions.

Therefore:

$$C_3 = 0 \quad (28)$$

According to eq. (28), the eq. (27) can be simplified as:

$$\begin{aligned}
u_r = \frac{r^{-n} \sin \varphi}{2nS_{33}} & \left[2C_2 \left(-S_{13} \bar{S}_{31} + (n-1) S_{23} \bar{S}_{31} + S_{33} \left(\bar{S}_{32} - n \bar{S}_{32} + \bar{S}_{33} \right) \right) - \right. \\
& 2C_1 r^{2n} \left(S_{13} \bar{S}_{31} + (n+1) S_{23} \bar{S}_{31} - S_{33} \left(\bar{S}_{32} + n \bar{S}_{32} + \bar{S}_{33} \right) \right) + \\
& \left. Anr^{n+2} \left(S_{33} \bar{S}_{31} + g \left(-\bar{S}_{31} (S_{13} + 3S_{23}) + S_{33} \left(3\bar{S}_{32} + \bar{S}_{33} \right) \right) \right) \right] + \\
& + F(\varphi)
\end{aligned} \tag{29}$$

where $F(\varphi)$ is an unknown function of φ . Substitution of eqs. (19) and (29) with eq. (23) yields:

$$\begin{aligned}
u_\varphi = G(r) + \int F(\varphi) d\varphi + \\
\frac{r^{-n} \cos \varphi}{2nS_{33}} & \left[2C_1 r^{2n} \left(n^2 \left(S_{23} \bar{S}_{21} - S_{33} \bar{S}_{22} \right) - \bar{S}_{31} (S_{13} + S_{23}) + \right. \\
& n \left(\bar{S}_{21} (S_{13} + S_{23}) - S_{23} \bar{S}_{31} - S_{33} \left(\bar{S}_{22} + \bar{S}_{23} + \bar{S}_{32} \right) \right) + \\
& \left. S_{33} \left(\bar{S}_{32} + \bar{S}_{33} \right) \right) + \\
& 2C_2 \left(n^2 \left(S_{23} \bar{S}_{21} - S_{33} \bar{S}_{22} \right) - \bar{S}_{31} (S_{13} + S_{23}) + \right. \\
& n \left(-\bar{S}_{21} (S_{13} + S_{23}) + S_{23} \bar{S}_{31} + S_{33} \left(\bar{S}_{22} + \bar{S}_{23} - \bar{S}_{32} \right) \right) + \\
& \left. S_{33} \left(\bar{S}_{32} + \bar{S}_{33} \right) \right) + \\
& Anr^{n+2} \left(S_{33} \left(\bar{S}_{31} - 2\bar{S}_{21} \right) + g \left((S_{13} + 3S_{23}) \left(2\bar{S}_{21} - \bar{S}_{31} \right) + \right. \right. \\
& \left. \left. S_{33} \left(-6\bar{S}_{22} - 2\bar{S}_{23} + 3\bar{S}_{32} + \bar{S}_{33} \right) \right) \right) \right]
\end{aligned} \tag{30}$$

where $G(r)$ is an unknown function of r .

Taking into account the condition of symmetry

$$u_\varphi(\varphi) = -u_\varphi(\pi - \varphi) \tag{31}$$

eq. (30) yields:

$$G(r) + \int F(\varphi) d\varphi = 0 \tag{32}$$

Let

$$\int F(\varphi) d\varphi = E(\varphi) \quad (33)$$

then eq. (28) can be written:

$$G(r) + E(\varphi) = 0 \quad (34)$$

yielding

$$G(r) = 0 \quad (35)$$

and

$$E(\varphi) = 0 \quad (36)$$

or

$$F(\varphi) = 0 \quad (37)$$

With the aid of eqs. (28), (35), (37) and using the following notations

$$\lambda_1 = -2 \left[S_{13} \bar{S}_{31} + (n+1) S_{23} \bar{S}_{31} - S_{33} \left(\bar{S}_{32} + n \bar{S}_{32} + \bar{S}_{33} \right) \right] r^{2n} \left(\frac{r^{-n}}{2nS_{33}} \right) \quad (38)$$

$$\lambda_2 = 2 \left[-S_{13} \bar{S}_{31} + (n-1) S_{23} \bar{S}_{31} + S_{33} \left(\bar{S}_{32} - n \bar{S}_{32} + \bar{S}_{33} \right) \right] \left(\frac{r^{-n}}{2nS_{33}} \right) \quad (39)$$

$$\lambda_3 = nr^{n+2} \left[S_{33} \bar{S}_{31} + g \left(-\bar{S}_{31} (S_{13} + 3S_{23}) + S_{33} \left(3\bar{S}_{32} + \bar{S}_{33} \right) \right) \right] \left(\frac{r^{-n}}{2nS_{33}} \right) \quad (40)$$

$$\begin{aligned} \lambda_4 = 2r^{2n} & \left[n^2 \left(S_{23} \bar{S}_{21} - S_{33} \bar{S}_{22} \right) - \bar{S}_{31} (S_{13} + S_{23}) + \right. \\ & n \left(\bar{S}_{21} (S_{13} + S_{23}) - S_{23} \bar{S}_{31} - S_{33} \left(\bar{S}_{22} + \bar{S}_{23} + \bar{S}_{32} \right) \right) + \\ & \left. S_{33} \left(\bar{S}_{32} + \bar{S}_{33} \right) \right] \left(\frac{r^{-n}}{2nS_{33}} \right) \end{aligned} \quad (41)$$

$$\begin{aligned} \lambda_5 = 2 & \left[n^2 \left(S_{23} \bar{S}_{21} - S_{33} \bar{S}_{22} \right) - \bar{S}_{31} (S_{13} + S_{23}) + \right. \\ & n \left(-\bar{S}_{21} (S_{13} + S_{23}) + S_{23} \bar{S}_{31} + S_{33} \left(\bar{S}_{22} + \bar{S}_{23} - \bar{S}_{32} \right) \right) + \\ & \left. S_{33} \left(\bar{S}_{32} + \bar{S}_{33} \right) \right] \left(\frac{r^{-n}}{2nS_{33}} \right) \end{aligned} \quad (42)$$

$$\lambda_6 = nr^{n+2} \left\{ S_{33} \left(\bar{S}_{31} - 2\bar{S}_{21} \right) + g \left[\left(S_{13} + 3S_{23} \right) \left(2\bar{S}_{21} - \bar{S}_{31} \right) + S_{33} \left(-6\bar{S}_{22} - 2\bar{S}_{23} + 3\bar{S}_{32} + \bar{S}_{33} \right) \right] \right\} \left(\frac{r^{-n}}{2nS_{33}} \right) \quad (43)$$

the expressions (29), (30) can be written:

$$u_r = \sin \varphi (\lambda_1 C_1 + \lambda_2 C_2 + \lambda_3 A) \quad (44)$$

$$u_\varphi = \cos \varphi (\lambda_4 C_1 + \lambda_5 C_2 + \lambda_6 A) \quad (45)$$

With the aid of eq. (28) and using the following notations

$$\mu_1 = r^{n-1} \quad (46)$$

$$\mu_2 = -r^{-n-1} \quad (47)$$

$$\mu_3 = gr \quad (48)$$

$$\mu_4 = (n+1)r^{n-1} \quad (49)$$

$$\mu_5 = (n-1)r^{-n-1} \quad (50)$$

$$\mu_6 = -(S_{13} + S_{23} + nS_{23})r^{n-1} \quad (51)$$

$$\mu_7 = (S_{13} + S_{23} - nS_{23})r^{-n-1} \quad (52)$$

$$\mu_8 = (S_{33} - S_{13}g - 3S_{23}g)r \quad (53)$$

the expressions (1)-(4) can be written:

$$\sigma_r = \sin \varphi (\mu_1 C_1 + \mu_2 C_2 + \mu_3 A) \quad (54)$$

$$\sigma_\varphi = \sin \varphi (\mu_4 C_1 + \mu_5 C_2 + 3\mu_3 A) \quad (55)$$

$$\sigma_z = \frac{\sin \varphi}{S_{33}} (\mu_6 C_1 + \mu_7 C_2 + \mu_8 A) \quad (56)$$

$$\tau_{r\varphi} = -\cos \varphi (\mu_1 C_1 + \mu_2 C_2 + \mu_3 A) \quad (57)$$

3.2. Multi-layered pipe

The equations (1)-(4) and (44), (45) express the stresses and deformations for a single-layered pipe. For the dimensioning of a multi-layered pipe under bending (Figure 7), we have to determine the stresses σ_r , σ_θ , σ_z , $\tau_{r\theta}$ for each layer k . Therefore, the next step is the determination of the unknown constants C_1 , C_2 , A for all layers from $k=1$ to $k=N$. To achieve this target, the following conditions have to be satisfied:

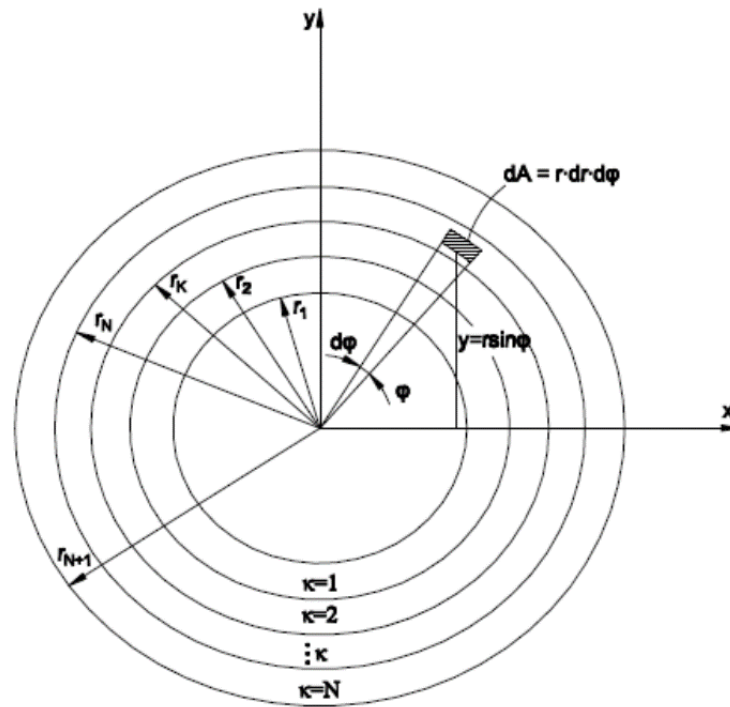


Figure 7. Geometry of a cross section of a multi-layered pipe

1) Equilibrium equations on interfaces

$$\left. \begin{aligned}
 \tau_{r\phi}^1(r_2) &= \tau_{r\phi}^2(r_2) \\
 \tau_{r\phi}^2(r_3) &= \tau_{r\phi}^3(r_3) \\
 &\dots\dots\dots \\
 &\dots\dots\dots \\
 &\dots\dots\dots \\
 \tau_{r\phi}^k(r_{k+1}) &= \tau_{r\phi}^{k+1}(r_{k+1}) \\
 &\dots\dots\dots \\
 &\dots\dots\dots \\
 &\dots\dots\dots \\
 \tau_{r\phi}^{N-1}(r_N) &= \tau_{r\phi}^N(r_N)
 \end{aligned} \right\} \begin{array}{l} \\ \\ \\ \\ (N-1) \text{ conditions} \\ \\ \\ \end{array} \quad (58)$$

2) Compatibility equations

$$\left. \begin{aligned}
 u_r^1(r_2) &= u_r^2(r_2) \\
 u_r^2(r_3) &= u_r^3(r_3) \\
 &\dots\dots\dots \\
 &\dots\dots\dots \\
 &\dots\dots\dots \\
 u_r^k(r_{k+1}) &= u_r^{k+1}(r_{k+1}) \\
 &\dots\dots\dots \\
 &\dots\dots\dots \\
 &\dots\dots\dots \\
 u_r^{N-1}(r_N) &= u_r^N(r_N)
 \end{aligned} \right\} \quad (N-1) \text{ conditions} \quad (59)$$

$$\left. \begin{aligned}
 u_\phi^1(r_2) &= u_\phi^2(r_2) \\
 u_\phi^2(r_3) &= u_\phi^3(r_3) \\
 &\dots\dots\dots \\
 &\dots\dots\dots \\
 &\dots\dots\dots \\
 u_\phi^k(r_{k+1}) &= u_\phi^{k+1}(r_{k+1}) \\
 &\dots\dots\dots \\
 &\dots\dots\dots \\
 &\dots\dots\dots \\
 u_\phi^{N-1}(r_N) &= u_\phi^N(r_N)
 \end{aligned} \right\} \quad (N-1) \text{ conditions} \quad (60)$$

3) Boundary conditions on exterior cylindrical surfaces

The conditions on the exterior surfaces of the pipe located on $r=rI$ and $r=rN+I$ are:

$$\left. \begin{aligned}
 \tau_{r\phi}^1(r_1) &= 0 \\
 \tau_{r\phi}^N(r_{N+1}) &= 0
 \end{aligned} \right\} \quad 2 \text{ conditions} \quad (61)$$

4) Boundary conditions on the cross sections at the ends of the pipe

Due to the action of stress $\sigma_z^k(r, \phi)$ on an elementary area $dA = r d\phi dr$ located within an arbitrary layer k (Figure 7), the corresponding elementary load is $dN_z = \sigma_z^k(r, \phi).rd\phi.dr$. This axial force yields an elementary bending moment $dM^k = ydN$, where $y = r \sin \phi$. Therefore, the bending moment due to the cross section of a layer k is $M_k = 2 \int \int \sigma_z^k(r, \phi) r^2 \sin \phi dr d\phi$. With the aid of the last equation the equilibrium between the bending moment M acting at the ends of pipe is equal to the summation of the bending moments due to N layers, i.e. $M = \sum_{\kappa=1}^N M_\kappa$ or

With the aid of eq. (44) the conditions (59) for a multi-layered pipe with stacking sequence $(\pm\theta)_{NP}$ yield:

$$\left. \begin{aligned} \lambda_1(r_2,1)C_1^1 + \lambda_2(r_2,1)C_2^1 + \lambda_3(r_2,1)A^1 &= \lambda_1(r_2,2)C_1^2 + \lambda_2(r_2,2)C_2^2 + \lambda_3(r_2,2)A^2 \\ \lambda_1(r_3,2)C_1^2 + \lambda_2(r_3,2)C_2^2 + \lambda_3(r_3,2)A^2 &= \lambda_1(r_3,3)C_1^3 + \lambda_2(r_3,3)C_2^3 + \lambda_3(r_3,3)A^3 \\ \dots & \\ \dots & \\ \lambda_1(r_{k+1},k)C_1^k + \lambda_2(r_{k+1},k)C_2^k + \lambda_3(r_{k+1},k)A^k &= \lambda_1(r_{k+1},k+1)C_1^{k+1} + \lambda_2(r_{k+1},k+1)C_2^{k+1} + \lambda_3(r_{k+1},k+1)A^{k+1} \\ \dots & \\ \dots & \\ \lambda_1(r_N,N-1)C_1^{N-1} + \lambda_2(r_N,N-1)C_2^{N-1} + \lambda_3(r_N,N-1)A^{N-1} &= \lambda_1(r_N,N)C_1^N + \lambda_2(r_N,N)C_2^N + \lambda_3(r_N,N)A^N \end{aligned} \right\} \quad (71)$$

Similarly, with the aid of eq. (45), the conditions (60) can be written:

$$\left. \begin{aligned} \lambda_4(r_2,1)C_1^1 + \lambda_5(r_2,1)C_2^1 + \lambda_6(r_2,1)A^1 &= \lambda_4(r_2,2)C_1^2 + \lambda_5(r_2,2)C_2^2 + \lambda_6(r_2,2)A^2 \\ \lambda_4(r_3,2)C_1^2 + \lambda_5(r_3,2)C_2^2 + \lambda_6(r_3,2)A^2 &= \lambda_4(r_3,3)C_1^3 + \lambda_5(r_3,3)C_2^3 + \lambda_6(r_3,3)A^3 \\ \dots & \\ \dots & \\ \lambda_4(r_{k+1},k)C_1^k + \lambda_5(r_{k+1},k)C_2^k + \lambda_6(r_{k+1},k)A^k &= \lambda_4(r_{k+1},k+1)C_1^{k+1} + \lambda_5(r_{k+1},k+1)C_2^{k+1} + \lambda_6(r_{k+1},k+1)A^{k+1} \\ \dots & \\ \dots & \\ \lambda_4(r_N,N-1)C_1^{N-1} + \lambda_5(r_N,N-1)C_2^{N-1} + \lambda_6(r_N,N-1)A^{N-1} &= \lambda_4(r_N,N)C_1^N + \lambda_5(r_N,N)C_2^N + \lambda_6(r_N,N)A^N \end{aligned} \right\} \quad (72)$$

The above equations (70)-(72) regarding the interfaces of the layers have to be completed with the boundary conditions on exterior surfaces of the multi-layered pipe. Taking into account the eq. (57), the conditions (61) yield:

$$\left. \begin{aligned} \mu_1(r_1,1)C_1^1 + \mu_2(r_1,1)C_2^1 + \mu_3(r_1,1)A^1 &= 0 \\ \mu_1(r_N,N-1)C_1^N + \mu_2(r_N,N-1)C_2^N + \mu_3(r_N,N-1)A^N &= 0 \end{aligned} \right\} \quad (73)$$

The equations (70)-(73) as well as the eq. (63) can be written in the following matrix form:

$$\begin{bmatrix} [M_1] & [M_2] & [M_3] \\ [\Lambda_1] & [\Lambda_2] & [\Lambda_3] \\ [\Lambda_4] & [\Lambda_5] & [\Lambda_6] \\ [B_1] & [B_2] & [B_3] \\ [J_6] & [J_7] & [J_8] \end{bmatrix} \begin{Bmatrix} \{C_1\} \\ \{C_2\} \\ \{A\} \end{Bmatrix} = \{L\} \quad (74)$$

where: $\{C_1\} = \{C_1^1, C_1^2, C_1^3, \dots, C_1^k, \dots, C_1^N\}^T$ (75)

$$\{C_2\} = \{C_2^1, C_2^2, C_2^3, \dots, C_2^k, \dots, C_2^N\}^T \quad (76)$$

$$\{A\} = \{A^1, A^2, A^3, \dots, A^k, \dots, A^N\}^T \quad (77)$$

$$[M_i]_{(N-1) \times N} = \begin{bmatrix} \mu_i(2,1) & -\mu_i(2,2) & 0 & 0 & 0 & 0 & 0 & 0 & 0 & 0 \\ 0 & \mu_i(3,2) & -\mu_i(3,3) & 0 & 0 & 0 & 0 & 0 & 0 & 0 \\ 0 & 0 & \mu_i(4,3) & -\mu_i(4,4) & 0 & 0 & 0 & 0 & 0 & 0 \\ 0 & 0 & 0 & 0 & \ddots & 0 & 0 & 0 & 0 & 0 \\ 0 & 0 & 0 & 0 & 0 & \mu_i(k,k-1) & -\mu_i(k,k) & 0 & 0 & 0 \\ 0 & 0 & 0 & 0 & 0 & 0 & 0 & \ddots & 0 & 0 \\ 0 & 0 & 0 & 0 & 0 & 0 & 0 & 0 & \mu_i(N,N-1) & -\mu_i(N,N) \end{bmatrix} \quad (78)$$

$$[\Lambda_i]_{(N-1) \times N} = \begin{bmatrix} \lambda_i(2,1) & -\lambda_i(2,2) & 0 & 0 & 0 & 0 & 0 & 0 & 0 & 0 \\ 0 & \lambda_i(3,2) & -\lambda_i(3,3) & 0 & 0 & 0 & 0 & 0 & 0 & 0 \\ 0 & 0 & \lambda_i(4,3) & -\lambda_i(4,4) & 0 & 0 & 0 & 0 & 0 & 0 \\ 0 & 0 & 0 & 0 & \ddots & 0 & 0 & 0 & 0 & 0 \\ 0 & 0 & 0 & 0 & 0 & \lambda_i(k,k-1) & -\lambda_i(k,k) & 0 & 0 & 0 \\ 0 & 0 & 0 & 0 & 0 & 0 & 0 & \ddots & 0 & 0 \\ 0 & 0 & 0 & 0 & 0 & 0 & 0 & 0 & \lambda_i(N,N-1) & -\lambda_i(N,N) \end{bmatrix} \quad (79)$$

$$[B_i]_{2 \times N} = \begin{bmatrix} \mu_i(1,1) & 0 & 0 & 0 & 0 & 0 & 0 & 0 & 0 & 0 \\ \mu_i(N,N-1) & 0 & 0 & 0 & 0 & 0 & 0 & 0 & 0 & 0 \end{bmatrix} \quad (80)$$

$$\{J_i\}_{1 \times N} = \{I_i^1 \quad I_i^2 \quad I_i^3 \quad \dots \quad I_i^{k-1} \quad I_i^k \quad I_i^{k+1} \quad \dots \quad I_i^{N-1} \quad I_i^N\} \quad (81)$$

$$\{L\}_{3 \times 1} = \left\{ 0 \quad 0 \quad 0 \quad 0 \quad 0 \quad 0 \quad 0 \quad 0 \quad 0 \quad \frac{M}{\pi} \right\}^T \quad (82)$$

C_1^k is the coefficient C_1 for the k-th layer

C_2^k is the coefficient C_2 for the k-th layer

A^k is the coefficient A for the k-th layer

$\mu_i(j,k)$ is the coefficient μ_i for the k-th layer for $r = r_j$

$\lambda_i(j,k)$ is the coefficient λ_i for the k-th layer for $r = r_j$

I_i^k is the coefficient I_i for the k-th layer.

The solution of the matrix equation (74) yields the unknown constants C_1^k, C_2^k, A^k ($k = 1, 2, \dots, NP$) for all layers. Therefore, using the values $C_1^{NP}, C_2^{NP}, A^{NP}$ of the critical exterior layer ($k = NP$), its stress state can now be determined by the Eqs. (1)-(4). In that case, the determination of the principal stresses $\sigma_1, \sigma_2, \tau_{12}$ of the exterior layer is possible by using eq. (70). Finally, the allowable bending moment can now be obtained by using a failure criterion (e.g. [10]).

4. Implementation of the method to typical examples

Taking into account the described model, the allowable values of bending moment M have been estimated for multilayered pipes made by E-Glass/Epoxy material [14]. The results are demonstrated in Figures 8(a)-(e). The calculations have been performed with the aid of the standard software "Mathematica" [15]. Trying several values of M , the program calculates the value of the Tsai-Wu expression. The value of M yielding unit value for the Tsai-Wu expression is the bending capacity of the multilayered pipe. In the derived diagrams are demonstrated the allowable values M for pipes of diameters $Dia = 0.10 \text{ m}, \dots, 1.2 \text{ m}$ consisting of plies of thickness 0.150 mm and fiber orientation $\theta = \pm 15^\circ, \pm 30^\circ, \dots, \pm 75^\circ$ for number of plies $NP = 10, \dots, 50$. The results are shown in Figures 8(a)-(e).

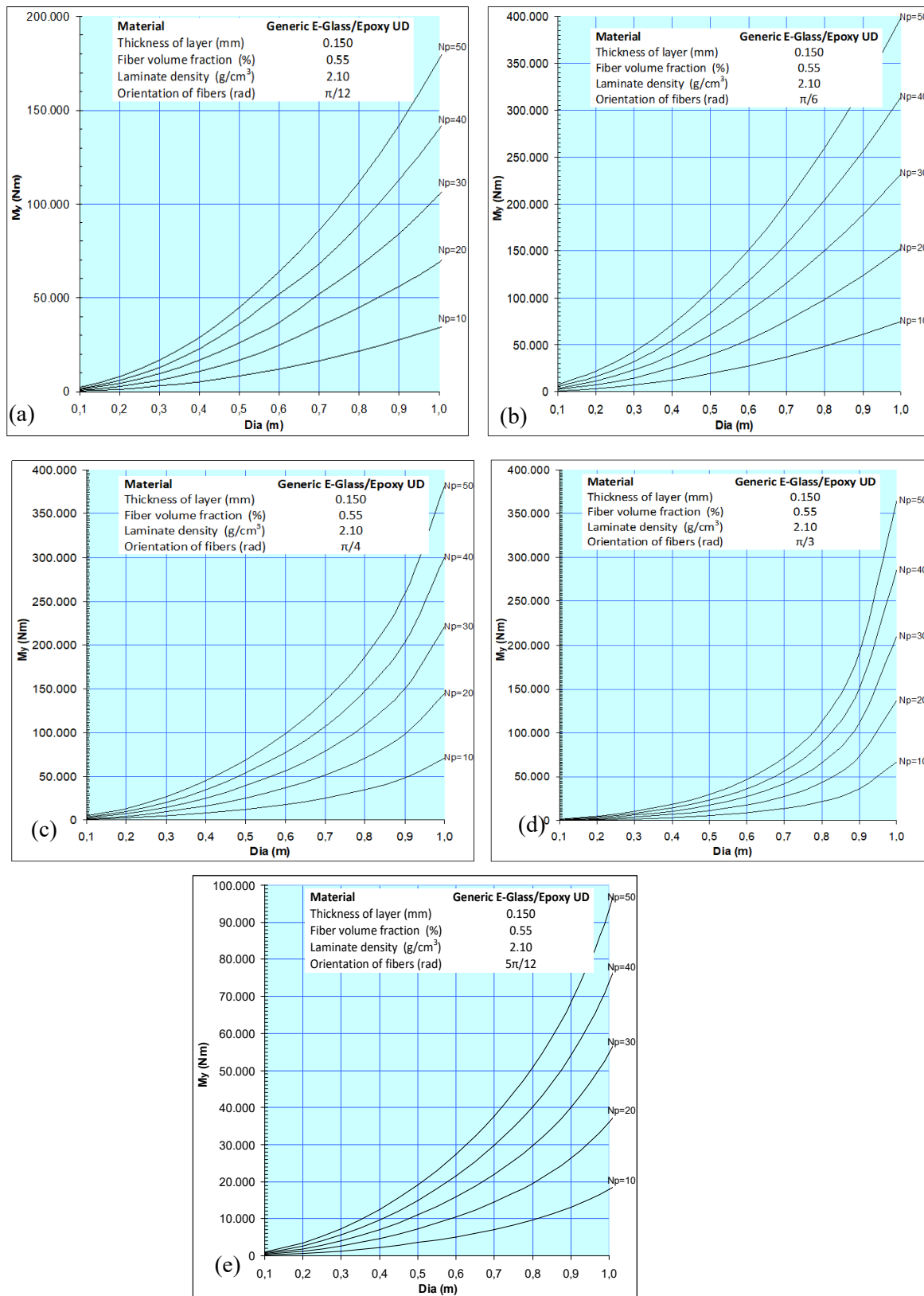


Figure 8. Bending capacity of multilayered E-Glass/Epoxy pipelines

5. Conclusions

1. In the present work, the bending of multilayered FRP pipelines during S-lay and J-lay offshore installation is analyzed.
2. With the aid of Lekhnitskii formalism for stresses of anisotropic materials, and taking into account the equilibrium equations of the layers, the compatibility and the boundary conditions on the interfaces, as well as the Tsai-Wu failure criterion, a mathematical model is derived for bending capacity during installation.
3. Unlike existing commercial software packages, the proposed analytical model is advantageous because it provides accurate results.
4. Implementation of the model on typical multilayered FRP pipelines made of E-Glass/Epoxy material has been carried out and useful nomographs for quick estimation of the bending capacity are provided.

References

- [1] Bai Y and Bai Q 2005 *Subsea pipelines and risers*, Elsevier.
- [2] B Reddy D V and Swamidas A S J 2014 *Essentials of offshore structures*, CRC press.
- [3] Pavlou D G 2007 *Computational and experimental analysis of damaged materials*, Transworld Research Network.
- [4] Guedes R M 2011 *Creep and fatigue in polymer matrix composites*, Woodhead publishing.
- [5] Harris B 2003 *Fatigue in composites*, CRC press.
- [6] Berenberg B <http://composite.about.com>.
- [7] Lekhnitskii S G 1963 *Theory of elasticity of an anisotropic elastic body*, Holden-Day.
- [8] Xia M, Takayanagi H and Kemmochi K 2002 Bending behavior of filament-wound fiber-reinforced sandwich pipes, *Compos Struct* **56**, 201-10.
- [9] Reddy J N 2004 *Mechanics of laminated composite plates and shells*, CRC press.
- [10] Tsai S W 1971 and Wu E M A general theory of strength for anisotropic materials, *Journal of Composite Materials* **5**, 58-80.
- [11] Flügge W 1973 *Stresses in shells*, Springer-Verlag.
- [12] Timoshenko S P and Gere J M 2009 *Theory of elastic stability*, Dover publications.
- [13] Kollár L P and Springer G S 2003 *Mechanics of composite structures*, Cambridge University Press.
- [14] Pavlou D G 2013, *Composite Materials in Piping Applications*, Destech publications.
- [15] Wolfram Mathematica, *Mathematica user manual*, <https://www.wolfram.com/mathematica/>.